ELSEVIER

Nuclear Physics A 634 (1998) 41–56

NUCLEAR PHYSICS A

Effective interactions and shell model studies of heavy tin isotopes

A. Holt [a], T. Engeland [a], M. Hjorth-Jensen [b], E. Osnes [a]

[a] *Department of Physics, University of Oslo, N-0316 Oslo, Norway*
[b] *Nordita, Blegdamsvej 17, DK-2100 København Ø, Denmark*

Received 28 October 1997; revised 2 February 1998; accepted 17 February 1998

Abstract

We calculate the low-lying spectra of heavy tin isotopes from $A = 120$ to $A = 130$ using the $2s1d0g_{7/2}0h_{11/2}$ shell to define the model space. An effective interaction has been derived using ^{132}Sn as closed core employing perturbative many-body techniques. We start from a nucleon–nucleon potential derived from modern meson exchange models. This potential is in turn renormalized for the given medium, ^{132}Sn, yielding the nuclear reaction matrix, which is then used in perturbation theory to obtain the shell model effective interaction. © 1998 Elsevier Science B.V.

PACS: 21.60.-n; 21.60.Cs; 24.10.Cn; 27.60.+j
Keywords: Shell model; Effective interactions

1. Introduction

The tin isotopes offer a unique opportunity for examining the microscopic foundation of various phenomenological nuclear models. In the Sn isotopes, ranging from mass number $A = 100$ to $A = 132$, neutrons are filling the subshells between the magic numbers 50 and 82, and thus it is possible to examine how well proton-shell closure at mass number 50 is holding up as valence neutrons are being added, how collective features are developing, the importance of certain many-body effects, etc. Though, one of the problems in theoretical calculations of properties of light tin isotopes is the fact that the single-particle energies of ^{101}Sn are not known. This reduces the predictive power of theoretically calculated interactions to be used in the spectroscopy of light tin isotopes. For ^{131}Sn however, the single-particle energies are known [1], a fact which allows one to discriminate between various effective interactions.

Recently, several theoretical results have been presented for the light tin isotopes [2–7], however, for the heavy tin isotopes, only few microscopic calculations are available.

PII S0375-9474(98)00146-8

In Ref. [8] Insolia et al. study the spectra of odd and even isotopes in the framework of a multistep shell model BCS formalism, using matrix elements for the effective interaction extrapolated from those in the lead mass region [9].

The aim of this work is to derive a more appropriate effective interaction for heavy tin isotopes and perform extensive shell model studies of the isotopes from ^{120}Sn to ^{130}Sn. The effective neutron–hole interaction is calculated with respect to ^{132}Sn as a closed shell core, with a model space which includes the orbitals $2s_{1/2}$, $1d_{5/2}$, $1d_{3/2}$, $0g_{7/2}$ and $0h_{11/2}$. The perturbative many-body scheme employed to calculate such an effective interaction starts with the free nucleon–nucleon interaction. This interaction is in turn renormalized taking into account the specific nuclear medium. The medium renormalized potential, the so-called *G*-matrix, is then employed in a perturbative many-body scheme, as detailed in Ref. [5] and reviewed in the next section.

This work falls in four sections. In Section 2 we first describe how to calculate an effective interaction appropriate for heavy tin isotopes, using perturbative many-body techniques, and at the end give a brief presentation of the basis for the shell model calculation. The discussion of the results for both even and odd isotopes are given in Section 3, and concluding remarks are drawn in Section 4.

2. Effective interaction and shell model calculations

The aim of microscopic nuclear structure calculations is to derive various properties of finite nuclei from the underlying hamiltonian describing the interaction between nucleons. When dealing with nuclei, such as the heavy tin isotopes with $A \sim 132$, the full dimensionality of the many-body Schrödinger equation for an A-nucleon system

$$H\Psi_i(1,\ldots,A) = E_i\Psi_1(1,\ldots,A), \tag{1}$$

becomes intractable and one has to seek viable approximations to Eq. (1). In Eq. (1) E_i and Ψ_i are the eigenvalues and eigenfunctions for a state i in the Hilbert space.

In nuclear structure calculations, one is normally only interested in solving Eq. (1) for certain low-lying states. It is then customary to divide the Hilbert space in a model space defined by the operator P

$$P = \sum_{i=1}^{d} |\psi_i\rangle \langle\psi_i| , \tag{2}$$

with d being the size of the model space, and an excluded space defined by the operator Q

$$Q = \sum_{i=d+1}^{\infty} |\psi_i\rangle \langle\psi_i| , \tag{3}$$

such that $PQ = 0$. The assumption then is that the components of these low-lying states can be fairly well reproduced by configurations consisting of a few particles and holes

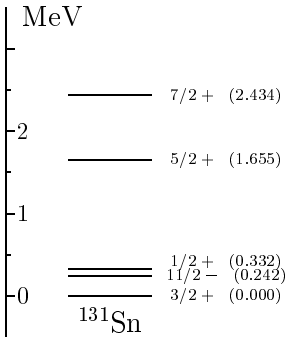

Fig. 1. Experimental single-hole energies for the orbits $2s_{1/2}$, $1d_{5/2}$, $1d_{3/2}$, $0g_{7/2}$ and $0h_{11/2}$ in ^{131}Sn.

occupying physically selected orbits. These selected orbitals define the model space. In the present work, the model space to be used both in the shell model calculation and the derivation of the effective interaction is given by the orbitals $2s_{1/2}$, $1d_{5/2}$, $1d_{3/2}$, $0g_{7/2}$ and $0h_{11/2}$. The single-particle energies, taken from Ref. [1], are displayed in Fig. 1.

Eq. (1) can then be rewritten as a secular equation

$$PH_{\text{eff}}P\Psi_i = P(H_0 + V_{\text{eff}})P\Psi_i = E_i P\Psi_i, \tag{4}$$

where H_{eff} now is an effective hamiltonian acting solely within the chosen model space. The term H_0 is the unperturbed hamiltonian while the effective interaction is given by

$$V_{\text{eff}} = \sum_{i=1}^{\infty} V_{\text{eff}}^{(i)}, \tag{5}$$

with $V_{\text{eff}}^{(1)}$, $V_{\text{eff}}^{(2)}$, $V_{\text{eff}}^{(3)}$,... being effective one-body, two-body, three-body interactions etc. It is also customary in nuclear shell model calculations to add the one-body effective interaction $V_{\text{eff}}^{(1)}$ to the unperturbed part of the hamiltonian so that

$$H_{\text{eff}} = \tilde{H}_0 + V_{\text{eff}}^{(2)} + V_{\text{eff}}^{(3)} + \ldots, \tag{6}$$

where $\tilde{H}_0 = H_0 + V_{\text{eff}}^{(1)}$. This allows us, as in the shell model, to replace the eigenvalues of $\tilde{H}_0$ by the empirical single-particle energies for the nucleon orbitals of our model space, or valence space, e.g. $2s_{1/2}$, $1d_{5/2}$, $1d_{3/2}$, $0g_{7/2}$ and $0h_{11/2}$, the valence neutron holes with respect to ^{132}Sn. Thus, the remaining quantity to calculate is the two- or more-body effective interaction $\sum_{i=2}^{\infty} V_{\text{eff}}^{(i)}$. In this work we will restrict our attention to the derivation of an effective two-body interaction

$$V_{\text{eff}} = V_{\text{eff}}^{(2)}, \tag{7}$$

using the many-body methods discussed in Ref. [5] and reviewed below. The study of effective three-body forces will be deferred to a later work [10].

Our scheme to obtain an effective hole–hole interaction appropriate for heavy tin isotopes starts with a free nucleon–nucleon interaction $V^{(2)}$ which is appropriate for

nuclear physics at low and intermediate energies. At present, there are several potentials available. The most recent versions of Machleidt and co-workers [11], the Nimjegen group [12] and the Argonne group [13] have a χ^2 per datum close to 1. In this work we will thus choose to work with the charge-dependent version of the Bonn potential models, see Ref. [11]. The potential model of Ref. [11] is an extension of the one-boson-exchange models of the Bonn group [14], where mesons like π, ρ, η, δ, ω and the fictitious σ meson are included. In the charge-dependent version of Ref. [11], the first five mesons have the same set of parameters for all partial waves, whereas the parameters of the σ meson are allowed to vary.

The next step in our perturbative many-body scheme is to handle the fact that the repulsive core of the nucleon–nucleon potential V (herafter, we let V stand for the nucleon–nucleon potential $V^{(2)}$) is unsuitable for perturbative approaches. This problem is overcome by introducing the reaction matrix G given by the solution of the Bethe–Goldstone equation

$$G = V + V\frac{Q}{\omega - H_0}G, \tag{8}$$

where ω is the unperturbed energy of the interacting nucleons, and H_0 is the unperturbed hamiltonian. The operator Q, commonly referred to as the Pauli operator, is a projection operator which prevents the interacting nucleons from scattering into states occupied by other nucleons. In this work we solve the Bethe–Goldstone equation for five starting energies ω, by way of the so-called double-partitioning scheme discussed in e.g. Ref. [5]. The G-matrix is the sum over all ladder type of diagrams. This sum is meant to renormalize the repulsive short-range part of the interaction. The physical interpretation is that the particles must interact with each other an infinite number of times in order to produce a finite interaction. To construct the Pauli operator which defines G, one has to take into account that neutrons and protons have different closed shell cores, $N = 82$ and $Z = 50$, respectively. This means that neutrons in the $2s1d0g_{7/2}0h_{11/2}$ shell are holes, while protons in the $2s1d0g_{7/2}0h_{11/2}$ shell are particles. For protons the Pauli operator must be constructed so as to prevent scattering into intermediate states with a single proton in any of the states defined by the orbitals from the $0s$ shell up to the $0g_{9/2}$ orbital. For a two-particle state with protons only, one has also to avoid scattering into states with two protons in the $2s1d0g$ ($0g_{9/2}$ excluded) and $2p1f0h$ shells. For neutrons one must prevent scattering into intermediate states with a single neutron in the orbitals from the $0s$ shell up to the $0h_{11/2}$ orbital. In addition, in the case of a two-particle state with neutrons only, one must prevent scattering into states with two neutrons in the $0h_{9/2}0i_{13/2}1f2p$ and $3s2d1g0i_{11/2}0j_{15/2}$ shells. If we have a proton–neutron two-particle state we must in addition prevent scattering into two-body states where a proton is in the $2s1d0g$ ($0g_{9/2}$ excluded) and $2p1f0h$ shells and a neutron is in the $0h_{9/2}0i_{13/2}1f2p$ and $3s2d1g0i_{11/2}0j_{15/2}$ shells.

A harmonic-oscillator basis was chosen for the single-particle wave functions, with an oscillator energy $\hbar\Omega$ given by $\hbar\Omega = 45A^{-1/3} - 25A^{-2/3} = 7.87$ MeV, $A = 132$ being the mass number.

Finally, we briefly sketch how to calculate an effective two-body interaction for the chosen model space in terms of the G-matrix. Since the G-matrix represents just the summmation to all orders of ladder diagrams with particle-particle diagrams, there are obviously other terms which need to be included in an effective interaction. Long-range effects represented by core-polarization terms are also needed. The first step then is to define the so-called $\hat{Q}$-box given by

$$P\hat{Q}P = PGP + P\left(G\frac{Q}{\omega - H_0}G + G\frac{Q}{\omega - H_0}G\frac{Q}{\omega - H_0}G + \ldots\right)P\,. \tag{9}$$

The $\hat{Q}$-box is made up of non-folded diagrams which are irreducible and valence linked. A diagram is said to be irreducible if between each pair of vertices there is at least one hole state or a particle state outside the model space. In a valence-linked diagram the interactions are linked (via fermion lines) to at least one valence line. Note that a valence-linked diagram can be either connected (consisting of a single piece) or disconnected. In the final expansion including folded diagrams as well, the disconnected diagrams are found to cancel out [15]. This corresponds to the cancellation of unlinked diagrams of the Goldstone expansion [15]. These definitions are discussed in Refs. [5,15]. We can then obtain an effective interaction $H_{\rm eff} = \tilde{H}_0 + V_{\rm eff}^{(2)}$ in terms of the $\hat{Q}$-box, with [5,15]

$$V_{\rm eff}^{(2)}(n) = \hat{Q} + \sum_{m=1}^{\infty}\frac{1}{m!}\frac{d^m\hat{Q}}{d\omega^m}\left\{V_{\rm eff}^{(2)}(n-1)\right\}^m, \tag{10}$$

where (n) and $(n-1)$ refer to the effective interaction after n and $n-1$ iterations. The zeroth iteration is represented by just the $\hat{Q}$-box. Observe also that the effective interaction $V_{\rm eff}^{(2)}(n)$ is evaluated at a given model space energy ω, as is the case for the G-matrix as well. Here we choose $\omega = -20$ MeV. Moreover, although $\hat{Q}$ and its derivatives contain disconnected diagrams, such diagrams cancel exactly in each order [15], thus yielding a fully connected expansion in e.g. Eq. (10). Less than 10 iterations were needed in order to obtain a numerically stable result. All non-folded diagrams through third-order in the interaction G are included. For further details, see Ref. [5].

The effective two-particle interaction can in turn be used in shell model calculations. The shell model problem requires the solution of a real symmetric $n\times n$ matrix eigenvalue equation

$$\tilde{H}\,|\Psi_k\rangle = E_k\,|\Psi_k\rangle\,, \tag{11}$$

with $k = 1,\ldots,K$. At present our basic approach to finding solutions to Eq. (11) is the Lanczos algorithm; an iterative method which gives the solution of the lowest eigenstates. This method was already applied to nuclear physics problems by Whitehead *et al.* in 1977. The technique is described in detail in Ref. [16], see also [2].

The eigenstates of Eq. (11) are written as linear combinations of Slater determinants in the m-scheme, distributing the N particles(holes) in all possible ways through the

Table 1
Number of basis states for the shell model calculation of the $N = 82$ isotones, with $1d_{5/2}$, $0g_{7/2}$, $1d_{3/2}$, $2s_{1/2}$ and $0h_{11/2}$ single particle orbitals

System	Dimension	System	Dimension	System	Dimension
^{130}Sn	36	^{125}Sn	108 297	^{120}Sn	6 210 638
^{129}Sn	245	^{124}Sn	323 682	^{119}Sn	9 397 335
^{128}Sn	1504	^{123}Sn	828 422	^{118}Sn	12 655 280
^{127}Sn	7451	^{122}Sn	1 853 256	^{117}Sn	15 064 787
^{126}Sn	31 124	^{121}Sn	3 609 550	^{116}Sn	16 010 204

single particle m-scheme orbitals of the model space, $2s_{1/2}$, $1d_{5/2}$, $1d_{3/2}$, $0g_{7/2}$ and $0h_{11/2}$. As seen in Table 1, the dimensionality n of the eigenvalue matrix $\tilde{H}$ is increasing with increasing number of valence holes, and for the Sn isotopes of interest it is up to $n \approx 2 \times 10^7$.

3. Results and discussions

In this section we present and discuss the shell model results for as many as 12 valence nucleons. The intention is to gain insight and draw conclusions regarding the effective interaction on basis of a spectroscopic analysis. The effective interaction is derived for a core with $N \neq Z$.

All experimental information in the present analysis is taken from the data base of the National Nuclear Data Centre at Brookhaven [17].

3.1. Even tin isotopes

We will here discuss the even Sn isotopes as a whole, and focus on the general spectroscopic trends. The results of the SM calculation are displayed in Tables 2–4. The energy eigenvalues are sorted according to the angular momentum assignment.

The stable energy spacing between the 0^+ ground state and the first excited 2^+ state, which is so characteristic for the Sn isotopes, is well reproduced in our shell model calculation. The yrast states, 4_1^+, 6_1^+, 8_1^+ and 10_1^+ tend to have slightly too high excitation energies. The calculated energies are 0.1–0.4 MeV higher than the experimental ones. Non-yrast states like 2_2^+ and 4_2^+ are again in beautiful agreement with experiment.

The agreement between the calculated and the experimental 5_1^- and 7_1^- states in ^{130}Sn is very satisfactory. Towards the middle of the shell the deviation between theory and experiment becomes larger. The experimental excitation energies of the 5_1^- and 7_1^- states increase slightly as approaching the middle of the shell. Our calculated energy levels do however increase too much and come out about 0.3 MeV too high in ^{120}Sn.

The 3^- data is not well established in ^{130}Sn and ^{128}Sn, but where a comparison is possible the calculated 3_1^- states come out 0.3–0.4 MeV higher than their experimental counterparts. The calculated 3_2^- states are also too high in excitation energy. It may be

Table 2
Low-lying states for ^{130}Sn and ^{128}Sn. Energies in MeV

^{130}Sn				^{128}Sn			
J_i^π	Exp.	J_i^π	Theory	J_i^π	Exp.	J_i^π	Theory
0^+	0.00	0_1^+	0.00	0^+	0.00	0_1^+	0.00
		0_2^+	2.11			0_2^+	2.33
		0_3^+	2.38			0_3^+	2.52
(2^+)	1.22	2_1^+	1.46	(2^+)	1.17	2_1^+	1.28
(2^+)	2.03	2_2^+	2.17	$(1,2)^+$	2.10	2_2^+	2.14
		2_3^+	2.46	$1,2^+$	2.26	2_3^+	2.52
(4^+)	2.00	4_1^+	2.39	(4^+)	2.00	4_1^+	2.18
(4^+)	3.42	4_2^+	3.23			4_2^+	2.84
(6^+)	2.26	6_1^+	2.64	$(6,7^-)$	2.38	6_1^+	2.53
(8^+)	2.34	8_1^+	2.72	$(7^+,8,9)$	2.41	8_1^+	2.66
(10^+)	2.44	10_1^+	2.80			10_1^+	2.80
$(3^-,4^+)$	2.49	3_1^-	3.44			3_1^-	3.11
$(3^-,4^+)$	4.22	3_2^-	4.67			3_2^-	3.25
(5^-)	2.09	5_1^-	2.19	(5^-)	2.12	5_1^-	2.27
(7^-)	1.95	7_1^-	2.03	(7^-)	2.09	7_1^-	2.28

Table 3
Low-lying states for ^{126}Sn and ^{124}S. Energies in MeV

^{126}Sn				^{124}Sn			
J_i^π	Exp.	J_i^π	Theory	J_i^π	Exp.	J_i^π	Theory
0^+	0.00	0_1^+	0.00	0^+	0.00	0_1^+	0.00
		0_2^+	2.20	(0^+)	2.13	0_2^+	2.30
		0_3^+	2.75	(0^+)	2.69	0_3^+	2.84
2^+	1.14	2_1^+	1.21	2^+	1.13	2_1^+	1.17
2^+	2.11	2_2^+	2.17	(2^+)	2.12	2_2^+	2.16
2^+	2.37	2_3^+	2.60	(2^+)	2.43	2_3^+	2.73
4^+	2.05	4_1^+	2.21	4^+	2.10	4_1^+	2.26
$2,3,4^+$	2.71	4_2^+	2.64	$(2,3,4)$	2.60	4_2^+	2.53
4^+	3.42	4_3^+	3.09	(4^+)	2.70	4_3^+	3.03
		6_1^+	2.61			6_1^+	2.70
		8_1^+	2.74	(8^+)	2.45	8_1^+	2.80
		10_1^+	2.77			10_1^+	2.85
3^-	2.72	3_1^-	3.04	3^-	2.61	3_1^-	2.97
3^-	4.77	3_2^-	3.21	(3^-)	3.01	3_2^-	3.35
5^-	2.16	5_1^-	2.36	5^-	2.21	5_1^-	2.46
5^-	2.89	5_2^-	2.76			5_2^-	2.84
7^-	2.22	7_1^-	2.48	7^-	2.33	7_1^-	2.63

of interest to note that in the neighbouring $N = 82$ isotones low-lying 3^- states are observed which cannot be reproduced by the shell model [18] and thus presumably are collective states. For the tin isotopes we obtain two 3^- states, which are somewhat too strongly excited, but it is likely that both states are represented by configurations within our model space.

Table 4
Low-lying states for ^{122}Sn and ^{120}Sn. Energies in MeV

^{122}Sn				^{120}Sn			
J_i^π	Exp.	J_i^π	Theory	J_i^π	Exp.	J_i^π	Theory
0^+	0.00	0_1^+	0.00	0^+	0.00	0_1^+	0.00
0^+	2.09	0_2^+	2.41	0^+	1.88	0_2^+	2.51
(0^+)	2.67	0_3^+	2.80	0^+	2.16	0_3^+	2.66
2^+	1.14	2_1^+	1.15	2^+	1.17	2_1^+	1.14
2^+	2.15	2_2^+	2.15	2^+	2.10	2_2^+	2.13
4^+	2.14	4_1^+	2.30	4^+	2.19	4_1^+	2.30
4^+	2.33	4_2^+	2.51	(4^+)	2.47	4_2^+	2.54
6^+	2.56	6_1^+	2.78			6_1^+	2.86
8^+	2.69	8_1^+	2.88	(8^+)	2.69	8_1^+	2.96
10^+	2.78	10_1^+	2.95			10_1^+	3.10
3^-	2.49	3_1^-	2.90	3^-	2.40	3_1^-	2.86
3^-	3.36	3_2^-	3.47	3^-	3.47	3_2^-	3.70
5^-	2.25	5_1^-	2.55	5^-	2.28	5_1^-	2.63
5^-	2.75	5_2^-	2.96	(5^-)	2.55	5_2^-	3.10
7^-	2.41	7_1^-	2.74	7^-	2.48	7_1^-	2.85

Excited 0^+ states are at present only observed in the tin isotopes with $N < 76$. Towards the middle of the $N = 50-82$ shell, the 0_2^+ state comes gradually lower in energy. It is worth mentioning that at midshell, in ^{116}Sn, 0_2^+ is the first excited state. The agreement between the calculated and the observed 0_2^+ state in ^{124}Sn is rather good. The deviation between our calculated 0_2^+ state and the observed first excited 0^+ state in ^{122}Sn and ^{120}Sn is 0.32 and 0.63 MeV, respectively. We do not manage to reproduce the trend with decreasing excitation energy of the first excited 0^+ state as approaching the middle of the shell.

Close to midshell low-lying 0^+ intruder states have been reported that are supposed to be predominantly proton core excitations. The first evidence for low-lying proton excitations across the $Z = 50$ gap was found in $^{108-118}$Sn by Fielding et al. [19]. Later, collective band structures have been identified by Bron et al. [20], bands which are assumed to be based on deformed proton configurations. Such states are however beyond the scope of the present model.

3.1.1. Generalized seniority for even isotopes

We will here make a comparison of the SM with the generalized seniority model [21]. The generalized seniority scheme is an extension of the seniority scheme, i.e., from involving only one single j-orbital, the model is generalized to involve a group of j-orbitals within a major shell. The generalized seniority scheme is a more simple model than the shell model since a rather limited number of configurations with a strictly defined structure are included, thus allowing a more direct physical interpretation. States with seniority $v = 0$ are by definition states where all particles are coupled in pairs. Seniority $v = 2$ states have one pair broken, seniority $v = 4$ states have two pairs broken,

etc. The generalized seniority scheme is suitable for describing semi-magic nuclei where pairing plays an important role. The pairing picture and the generalized seniority scheme have been important for the description and understanding of the tin isotopes. A typical feature of the seniority scheme is that the spacing of energy levels are independent of the number of valence particles. For the tin isotopes, not only the spacing between the ground state and the 2_1^+ state, but also the spacing beween the ground state and the 4_1^+ and 6_1^+ states is fairly constant throughout the whole sequence of isotopes. In fundamental works on generalized seniority by for instance Talmi [21], the tin isotopes have been used as one of the major test cases. It is also worth mentioning the classical work on pairing by Kisslinger and Sorensen [22].

If we by closer investigation and comparison of the SM wave function and the seniority states find that the most important components are accounted for by the seniority scheme, we can benefit from this and reduce the SM basis. This would be particularly useful when we want to do calculations on systems with a large number of valence particles.

The operator for creating a generalized seniority ($v = 0$) pair is

$$S^\dagger = \sum_j \frac{1}{\sqrt{2j+1}} \alpha_j \sum_{m \geqslant 0} (-1)^{j-m} b_{jm}^\dagger b_{j-m}^\dagger, \tag{12}$$

where $b_{jm}^\dagger$ is the creation operator for holes. The generalized senitority ($v = 2$) operator for creating a broken pair is given by

$$D_{J,M}^\dagger = \sum_{j \leqslant j'} (1 + \delta_{j,j'})^{-1/2} \beta_{j,j'} \langle jmj'm' \,|JM\rangle \, b_{jm}^\dagger b_{j'm'}^\dagger. \tag{13}$$

The coefficients α_j and $\beta_{jj'}$ are obtained from the ^{130}Sn ground state and the excited states, respectively.

We calculate the squared overlaps between the constructed generalized seniority states and our shell model states

$$\begin{aligned} &(v = 0) \;\; |\langle {}^A\mathrm{Sn(SM)}; 0^+ | (S^\dagger)^{\frac{n}{2}} |\tilde{0}\rangle|^2 , \\ &(v = 2) \;\; |\langle {}^A\mathrm{Sn(SM)}; J_i | D_{JM}^\dagger (S^\dagger)^{\frac{n}{2}-1} |\tilde{0}\rangle|^2 . \end{aligned} \tag{14}$$

The vacuum state $|\tilde{0}\rangle$ is the ^{132}Sn-core and n is the number of valence particles. These quantities tell to what extent the shell model states satisfy the pairing picture, or in other words, how well is generalized seniority conserved as a quantum number.

The squared overlaps are tabulated in Table 5, and vary generally from 0.95 to 0.75. As the number of valence particles increases the squared overlaps are gradually decreasing. The overlaps involving the 4^+ states show a fragmentation. In ^{128}Sn, the 4_1^+ (SM) state is mainly a seniority $v = 2$ state. As approaching the middle of the shell, the next state, 4_2^+, takes more and more over the structure of a seniority $v = 2$ state. The fragmentation of seniority over these two states can be understood from the fact that they are rather close in energy and therefore may have mixed structure.

Table 5
Seniority $v = 0$ overlap $|\langle {}^{A}\mathrm{Sn}; 0^{+}|(S^{\dagger})^{n/2}|\tilde{0}\rangle|^2$ and the seniority $v = 2$ overlaps $|\langle {}^{A}\mathrm{Sn}; J_f|D^{\dagger}_{JM}(S^{\dagger})^{\frac{n}{2}-1}|\tilde{0}\rangle|^2$ for the lowest-lying eigenstates of $^{128-120}$Sn

	$A = 128$	$A = 126$	$A = 124$	$A = 122$	$A = 120$
0^+_1	0.96	0.92	0.87	0.83	0.79
2^+_1	0.92	0.89	0.84	0.79	0.74
4^+_1	0.73	0.66	0.44	0.13	0.00
4^+_2	0.13	0.18	0.39	0.66	0.74
6^+_1	0.81	0.85	0.83	0.79	0.64

3.1.2. Effective charges and E2 transitions

In the literature there is some discussion concerning the effective charges to be used in B(E2) calculations. Fogelberg and Blomqvist have used an effective charge $e_{\mathrm{eff}} = 1.0e$ in their study of single-hole states in ^{131}Sn [1]. In a work on $\nu h_{11/2}$ subshell filling, Broda et al. [23] are assigning an effective neutron charge, $e_{\mathrm{eff}} = 0.88(4)e$, to the $h_{11/2}$ holes. State dependent effective charges can be derived along the same lines as the effective interaction. Preliminary calculations of the effective charges for this mass region by one of the authors, Ref. [24], have given values between $0.7e$ and $0.9e$ for the different valence particle states. However, in this work the state dependence has not been incorporated, but an average value $e_{\mathrm{eff}} = 0.8e$ has been used.

In the vicinity of the ^{132}Sn-core E2 transition data are rather scarce. Towards the middle of the shell, and more stable isotopes, data are available. The agreement between our calculated B(E2) values and experimental data is overall very good, see Table 6 and 7. In ^{122}Sn and ^{120}Sn several E2 transition rates are measured. The experimental $B(E2; 4^+_1 \rightarrow 2^+_1)$ and $B(E2; 2^+_1 \rightarrow 0^+_1)$ values are measured to be 10–20 W.u., which indicates that the states are of collective nature. We reproduce all these transitions exceptionally well. For the two nuclei there is also experimental information on the transition $0^+_2 \rightarrow 2^+_1$. In ^{122}Sn an upper limit, $B(E2; 2^+_1 \rightarrow 0^+_1) < 6.1$ W.u. is given, and in ^{120}S the transition is reported to be 18.6 W.u., i.e., strongly collective. The transition rates are very sensitive to the structure of the wave functions and thus can give us valuable information. We fail in reproducing these E2 transitions by several orders of magnitude, and from that we can conclude that our SM 0^+_2 wave functions do not have the correct structure. As mentioned in the previous subsection the SM does also have problems in reproducing the correct energy of these 0^+_2 states. The calculated energies are too high compared to their experimental counterparts.

The measured $B(E2; 7^-_1 \rightarrow 5^-_1)$ transition rates are all small, 0.29 W.u. in ^{126}Sn and reduced to 0.004 W.u. in ^{120}Sn. While the experimental transition rates decrease with the number of valence particles, our calculated transition rates increase from 0.085 W.u. in ^{126}Sn to 2.90 W.u. in ^{120}Sn. This may indicate some short-comings of our negative parity wave functions. We believe that is associated with the interplay between the $0h_{11/2}$ orbital and the other orbitals. Even small corrections may change such weak transitions.

Broda et al. [23] argue that an effective charge twice as large as the value for ^{130}Sn is needed in ^{116}Sn. This enhancement of the e_{eff} in the middle of the $N = 50-82$ shell

Table 6
E2 transitions for ^{130,128,126}Sn. Units in W.u.

	^{130}Sn		^{128}Sn		^{126}Sn	
Transition	SM	Exp.	SM	Exp	SM	Exp
$2_1^+ \to 0_1^+$	2.07		4.33		6.57	
$0_2^+ \to 2_1^+$	0.96		0.056		0.17	
$4_1^+ \to 2_1^+$	1.45		4.13		6.03	
$5_1^- \to 7_1^-$	1.18	1.4 (2)				
$7_1^- \to 5_1^-$					0.085	0.29 (5)
$10_1^+ \to 8_1^+$	0.35	0.38 (4)				

Table 7
E2 transitions for ^{124,122,120}Sn. Units in W.u.

	^{124}Sn		^{122}Sn		^{120}Sn	
Transition	SM	Exp	SM	Exp	SM	Exp
$2_1^+ \to 0_1^+$	8.70	9.0 (2)	10.6	10.7 (6)	12.0	16.9 (3)
$0_2^+ \to 2_1^+$	0.38		0.046	<6.1	0.007	18.6 (25)
$7_1^- \to 5_1^-$	0.64	0.11 (2)	1.80	0.0146 (21)	2.90	0.0040 (2)
$4_1^+ \to 2_1^+$	9.42		14.6	10.0 (14)	18.2	14.8 (21)

is interpreted as a consequence of additional configuration mixing, corresponding to polarization of the softer midshell core. Our E2 results for ^{122,120}Sn do however not indicate the need for any larger effective charge as approaching the middle of the shell.

3.2. Odd isotopes

The results for the odd nuclei $^{129-121}$Sn are tabulated in Tables 8–12. In addition, for each nucleus, some selected yrast states are displayed in Fig. 2.

Characteristic for all the odd isotopes studied in this work is that the $1/2_1^+$, $3/2_1^+$, $11/2_1^-$ states are nearly degenerate, and there is then a gap to the next states located about 0.6 MeV higher. This feature can be traced back to the single-hole spectrum where the single-hole orbitals $1d_{3/2}$, $0h_{11/2}$ and $2s_{1/2}$ are closely degenerate and well separated from the $1d_{5/2}$ and $0g_{7/2}$ orbitals. The three lowest-lying states in $^{129-121}$Sn are satisfactorily reproduced in our model. Due to the near degeneracy of these states we do not always get the states in the correct order, but the deviation between theory and experiment never exceeds 0.2 MeV.

Considering now the negative parity states, in addition to the $11/2_1^-$ state, which is the ground state in $^{127-123}$Sn and nearly degenerate with the ground state in ^{129}Sn, there are low-lying $7/2^-$ and $9/2^-$ states. These states can typically be constructed by coupling an odd number of $0h_{11/2}$ holes to an even number of $1d_{3/2}$ or $2s_{1/2}$ holes. To excite holes into the three orbitals mentioned here costs little energy, and from this simple picture

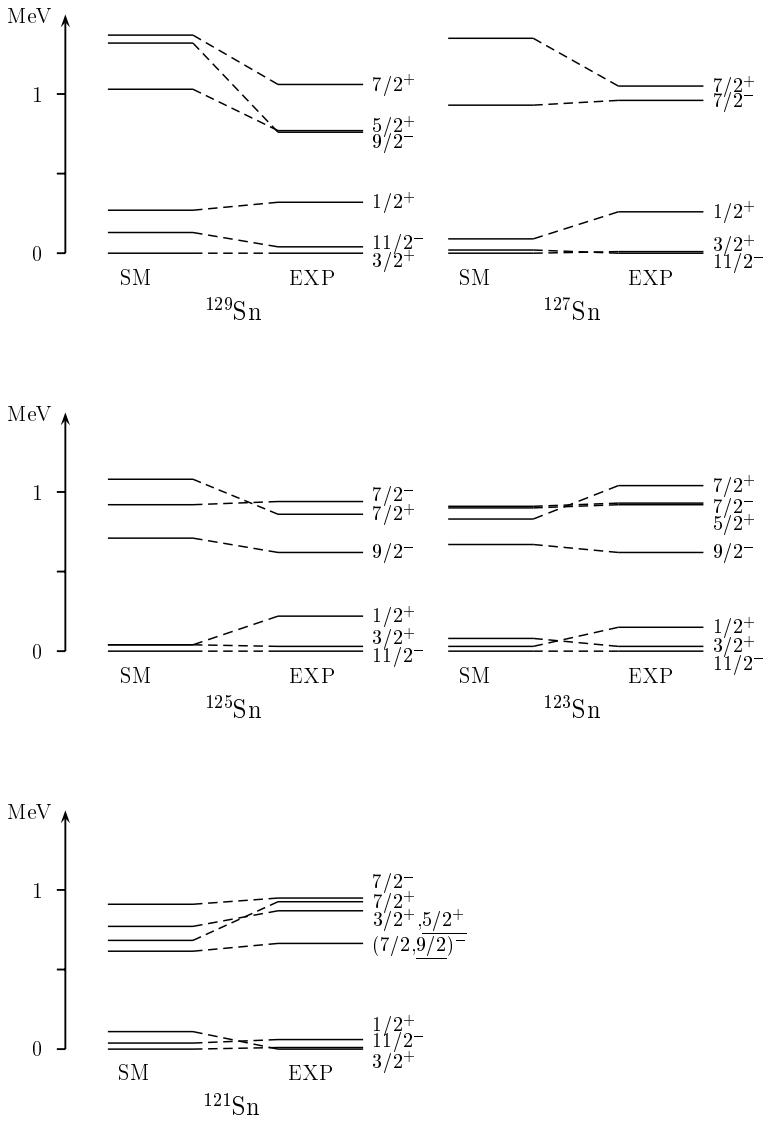

Fig. 2. Low-spin yrast states for $^{129-121}$Sn. Underlined spin assignments refer to the angular momentum of the SM states.

it is possible to understand the low energies of these states. The calculated $7/2_1^-$ state is in perfect agreement with experiment throughout the whole sequence of isotopes. We fail in reproducing the $9/2_1^-$ state in ^{129}Sn. In ^{127}Sn a comparison is difficult since the experimental $9/2_1^-$ state is not clearly identified. For the other isotopes the agreement between the calculated and the experimental $9/2_1^-$ state is good.

Table 8
Low-lying states for ^{129}Sn. Energies in MeV

^{129}Sn			
J_i^π	Exp.	J_i^π	Theory
$(3/2^+)$	0.00	$3/2_1^+$	0.00
$(11/2^-)$	0.04	$11/2_1^-$	0.13
$(1/2^+)$	0.32	$1/2_1^+$	0.27
$(9/2^-)$	0.76	$5/2_1^+$	1.03
$(5/2^+)$	0.77	$7/2_1^-$	1.05
$(7/2^-)$	1.04	$3/2_2^+$	1.22
$(7/2^+)$	1.06	$15/2_1^-$	1.28
$(1/2^+, 3/2^+)$	1.22	$9/2_1^-$	1.32
$(1/2^+, 3/2^+)$	1.29	$7/2_1^+$	1.37
$(7/2^+)$	1.87	$1/2_2^+$	1.43
$(7/2^+)$	2.12	$3/2_3^+$	1.45

Table 9
Low-lying states for ^{127}Sn. Energies in MeV

^{127}Sn			
J_i^π	Exp.	J_i^π	Theory
$(11/2^-)$	0.00	$3/2_1^+$	0.00
$(3/2^+)$	0.01	$11/2_1^-$	0.02
$(1/2^+)$	0.26	$1/2_1^+$	0.09
$(9/2^+, 11/2^+)$	0.65	$3/2_2^+$	0.86
$(7/2^+)$	0.81	$9/2_1^-$	0.86
$(3/2^+)$	0.95	$5/2_1^+$	0.89
$(7/2^-, 9/2, 11/2)$	0.96	$7/2_1^-$	0.93
$(7/2^+)$	1.05	$15/2_1^-$	1.11
$(1/2, 3/2)$	1.09	$5/2_2^+$	1.20
$(7/2^-, 9/2, 11/2)$	1.56	$1/2_2^+$	1.31
$(7/2^+)$	1.60	$3/2_3^+$	1.34
$(7/2, 9/2, 11/2^+)$	1.91	$7/2_1^+$	1.35
$(7/2^+)$	2.02	$13/2_1^-$	1.46

4. Summary and conclusions

A major aim of this work has been to provide a severe test of the foundation of the effective interaction. This is done by performing extensive shell model calculations over a large mass region. Most previous shell model calculations have been made for nuclei with only two or a few nucleons outside a closed-shell core. It is of interest to extend this test to systems with several valence nucleons. For this the Sn isotopes are particularly suitable. From the vicinity of the doubly magic ^{100}Sn to beyond the doubly magic ^{132}Sn experimental data is now available.

In this work we have investigated the range of heavy Sn isotopes between $A = 120$ and $A = 130$. These are described in terms of valence neutron holes with respect to the

Table 10
Low-lying states for ^{125}Sn. Energies in MeV

^{125}Sn			
J_i^π	Exp.	J_i^π	Theory
$11/2^-$	0.00	$11/2_1^-$	0.00
$3/2^+$	0.03	$1/2_1^+$	0.04
$1/2^+$	0.22	$3/2_1^+$	0.04
$(9/2^-)$	0.62	$9/2_1^-$	0.71
$7/2^+$	0.86	$3/2_2^+$	0.83
$1/2, 3/2$	0.93	$5/2_1^+$	0.89
$(7/2^-)$	0.94	$7/2_1^-$	0.92
$7/2^{(+)}$	1.06	$5/2_2^+$	1.06
$1/2, 3/2$	1.07	$15/2_1^-$	1.07
$(1/2^+, 3/2^+, 5/2^+)$	1.19	$7/2_1^+$	1.08
$(5/2)^+$	1.26	$1/2_2^+$	1.23
$7/2^+$	1.36	$3/2_3^+$	1.29
$(5/2)^+$	1.54	$13/2_1^-$	1.33

Table 11
Low-lying states for ^{123}Sn. Energies in MeV

^{123}Sn			
J_i^π	Exp.	J_i^π	Theory
$11/2^-$	0.00	$11/2_1^-$	0.00
$3/2^+$	0.03	$1/2_1^+$	0.03
$1/2^+$	0.15	$3/2_1^+$	0.08
$(9/2)^-$	0.62	$9/2_1^-$	0.67
$(3/2^+, 5/2^+)$	0.87	$7/2_1^+$	0.83
$5/2^+$	0.90	$3/2_2^+$	0.88
$(3/2)^+$	0.92	$7/2_1^-$	0.91
$7/2^-$	0.93	$5/2_1^+$	0.92
$(7/2)^+$	1.04	$5/2_2^+$	0.94
$(1/2, 3/2)^+$	1.07	$15/2_1^-$	1.05
$15/2^-$	1.11	$1/2_2^+$	1.21

^{132}Sn core. By and large, the essential spectroscopic properties are well described in our shell model scheme. In particular, it is gratifying that good results are obtained for nuclei far away from the ^{132}Sn core with respect to which the effective interaction and the single-particle energies are defined.

For the whole sequence of even isotopes the calculated $0^+ - 2^+$ spacing is approximately constant and in almost perfect agreement with experiment. The other yrast states tend however to be too highly excited. All negative parity states are slightly too high as well. The reason seems to be that there is too strong a coupling between holes in the $0h_{11/2}$ intruder orbital and holes in the other orbitals. Small adjustments of the $J = 0$ and 2 effective matrix elements $\langle n_j^2 | V_{\text{eff}} | 0h_{11/2}^2 \rangle_J$, where n_j are the orbitals $0g_{7/2}$, $1d_{5/2}$, $1d_{3/2}$ and $2s_{1/2}$, give results in better agreement with experiment.

Our shell model scheme has been greatly successful in describing the odd tin isotopes.

Table 12
Low-lying states for ^{121}Sn. Energies in MeV

^{121}Sn			
J_i^π	Exp.	J_i^π	Theory
$3/2^+$	0.00	$11/2_1^-$	0.00
$11/2^-$	0.01	$1/2_1^+$	0.04
$1/2^+$	0.06	$3/2_1^+$	0.11
$(7/2, 9/2)^-$	0.66	$9/2_1^-$	0.65
$3/2^+, 5/2^+$	0.87	$7/2_1^+$	0.68
$3/2^+, 5/2^+$	0.91	$5/2_1^+$	0.77
$7/2^+$	0.93	$7/2_1^-$	0.91
$(7/2)^-$	0.95	$3/2_2^+$	0.94
$3/2^+, 5/2^+$	1.10	$5/2_2^+$	0.98
$5/2^+$	1.12	$1/2_2^+$	1.24
$(5/2)^+$	1.15	$3/2_2^+$	1.24
$(7/2^+, 9/2^+)$	1.35	$7/2_2^+$	1.28
$(5/2)^+$	1.40	$5/2_3^+$	1.30

There is roughly a one-to-one correspondence between the calculated and experimental states below 1.0–1.5 MeV, and the states are generally in correct order. Usually, odd nuclei are more tricky to handle than the even nuclei, since they are more sensitive to the underlying structure, such as the single-particle energies and the interaction. However, in the present calculation we get at least as satisfactory results for the odd as for the even isotopes.

In summary we may conclude that the relative location of the states is satisfactory, but it ought to be mentioned that the absolute values of the binding energies are far off. As moving away from the closed $Z = 50$, $N = 82$ core, the systems become too strongly bound compared to experiment. The binding energy increases almost linearly with mass number A when going from ^{130}Sn to ^{120}Sn, whereas experimentally the binding energy saturates around ^{122}Sn. For example, the ten-particle system (^{122}Sn) is overbound by more than 7 MeV with the present effective interaction. Clearly, this seems to be a common problem to most effective interactions as pointed out by Zuker and co-workers [25]; one is not able to simultaneously achieve good spectroscopy and reproduction of the binding energy. Further investigations of this problem are clearly necessary. Left to be studied in more detail is the influence of three-body forces [10]. We would like to find out whether the three-body contributions will be of significant importance as the number of valence particles grows, and thus will bring the theoretical binding energies closer to the experimental values. Another explanation could be that the problems with reproduction of the binding energies may be ascribed to the two-body effective interaction itself and thus this ought to be subjected to further tests before definite conclusions can be drawn.

Acknowledgements

This work was initiated while one of us, M.H.J., was at the European Centre for Theoretical studies in Nuclear Physics and Related Areas, Trento, Italy. Financial support from the Instituto Trentino di Cultura, Trento, and the Research Council of Norway (NFR) is greatly acknowledged. The calculations have been carried out at the IBM cluster at the University of Oslo. Support for this from the NFR is acknowledged.

References

[1] B. Fogelberg and J. Blomqvist, Phys. Lett. B 137 (1984) 20.
[2] T. Engeland, M. Hjorth-Jensen, A. Holt and E. Osnes, Phys. Scripta T 56 (1995) 58.
[3] T. Engeland, M. Hjorth-Jensen, A. Holt and E. Osnes, Phys. Rev. C 48 (1993) R535.
[4] A. Holt, T. Engeland, M. Hjorth-Jensen and E. Osnes, Nucl. Phys. A 570 (1994) 137c.
[5] M. Hjorth-Jensen, T.T.S. Kuo and E. Osnes, Phys. Reports 261 (1995) 125.
[6] N. Sandulescu, J. Blomqvist and R.J. Liotta, Nucl. Phys. A 582 (1994) 257; Physica Scripta T56 (1995) 84.
[7] B.A. Brown and K. Rykaczewski, Phys. Rev. C 50 (1994) R2270.
[8] A. Insolia, N. Sandulescu, J. Blomqvist and R.J. Liotta, Nucl. Phys. A 550 (1992) 34.
[9] C. Pomar, J. Blomqvist, R.J. Liotta and A. Insolia, Nucl. Phys. A 515 (1990) 381.
[10] T. Engeland and M. Hjorth-Jensen, in preparation.
[11] R. Machleidt, F. Sammarruca and Y. Song, Phys. Rev. C 53 (1996)
[12] V.G.J. Stoks, R.A.M. Klomp, C.P.F. Terheggen and J.J. de Swart, Phys. Rev. C 48 (1993) 792.
[13] R.B. Wiringa, V.G.J. Stoks and R. Schiavilla, Phys. Rev. C 51 (1995) 38.
[14] R. Machleidt, Adv. Nucl. Phys. 19 (1989) 189.
[15] T.T.S. Kuo and E. Osnes, Folded-Diagram Theory of the Effective Interaction in Atomic Nuclei, Springer Lecture Notes in Physics, vol. 364 (Springer, Berlin, 1990).
[16] R.R. Whitehead, A. Watt, B.J. Cole and I. Morrison, Adv. Nucl. Phys. 9 (1977) 123.
[17] National Nuclear Data Centre, Brookhaven National Laboratory, Upton, N.Y., USA, http://www.nndc.bnl.gov/.
[18] A. Holt, T. Engeland, M. Hjorth-Jensen, E. Osnes and J. Suhonen, Nucl. Phys. A 618 (1997) 107.
[19] H. Fielding et al., Nucl. Phys. A 281 (1977) 389.
[20] J. Bron et al., Nucl. Phys. A 318 (1979) 335.
[21] I. Talmi, *in* Proc. Int. School of Physics "Enrico Fermi", Elementary Modes of Excitation in Nuclei, ed. A. Bohr and R.A. Broglia (North-Holland, Amsterdam, 1977) p. 352.
[22] L.S. Kisslinger and R.A. Sorensen, Mat. Fys. Medd. Dan. Vid. Selsk. 32, no. 9 (1960).
[23] R. Broda et al., Phys. Rev. Lett. 68 (1992) 1671.
[24] M. Hjorth-Jensen, unpublished.
[25] M. Dufour and A.P. Zuker, Phys. Rev. C 54 (1996) 1641;
A. Poves and A.P. Zuker, Phys. Rep. 70 (1981) 235; 71 (1981) 141.